



44<sup>TH</sup> TURBOMACHINERY & 31<sup>ST</sup> PUMP SYMPOSIA  
HOUSTON, TEXAS | SEPTEMBER 14 – 17 2015  
GEORGE R. BROWN CONVENTION CENTER

## A novel method for measurement and evaluation of torsional damping for geared turbomachinery during operation using lateral vibration probes

### **Stefano Morosi, Ph.D.**

Senior Consultant  
Lloyd's Register Consulting  
Denmark

### **Anders Crone**

Team Leader, Machinery Dynamics  
Lloyd's Register Consulting  
Sweden

### **Petter Pehrson**

Senior Consultant  
Lloyd's Register Consulting  
Denmark



*Dr. Stefano Morosi is a Senior Consultant in the Machinery Dynamics team at Lloyd's Register Consulting. His main duties include rotordynamic analysis and verification projects, field measurements, troubleshooting and root cause analyses, with particular focus on rotating and electromechanical systems. Stefano holds a PhD in Mechanical Engineering from the*

*Technical University of Denmark with a thesis focused on software and hardware prototyping of active control of high speed rotor bearing systems supported by a hybrid magnetic – gas bearing system.*



*Mr. Anders Crone is Team Leader for the Machinery Dynamics team of Lloyd's Register Consulting. His main work field is within rotor and machinery dynamics, machine integrity, condition monitoring and signal processing, in Oil & Gas, Renewables, Power and Industry. He holds an MSc in Mechanical Engineering from the Technical University of Denmark*



*Mr. Petter Pehrson is a Senior Consultant in the Machinery Dynamics team at Lloyd's Register consulting. He joined LR Consulting in 2011 were his main tasks include project management, measurement campaign and structural calculations within the Marine and Oil & Gas industry. He was awarded with his master thesis by the Royal Institute of Technology*

### **Staffan Lundholm**

Principal Consultant  
Lloyd's Register Consulting  
Sweden

### **Niklas Sehlstedt, Ph.D.**

Manager, Engineering Dynamics  
Lloyd's Register Consulting  
Sweden

*Stockholm in 2009 for work on dynamic loads on high speed vessels.*



*Mr. Staffan Lundholm is a Principal Consultant in the Machinery Dynamics team of Lloyd's Register Consulting. His main tasks include project management, measurement campaigns, computational verification and prediction of rotating equipment within the Oil & Gas industry. He was awarded with his master thesis by the Royal Institute of Technology Stockholm in 2007 for work on instability in rotating machinery caused by internal friction undertaken in collaboration with Lloyd's Register Consulting.*



*Dr. Niklas Sehlstedt is Department Manager for Engineering Dynamic. He first joined the company (then named ODS) in 2005 and worked as a machinery dynamics consultant for the oil and gas industry until joining Dresser-Rand in 2011 as the rotordynamics manager. He holds a Ph.D. in M.E. from Royal Institute of Technology in Stockholm, Sweden.*

### **ABSTRACT**

Measurement of the modal parameters of rotors is of interest to understand the dynamics of rotating systems, validate design models, and assess how operational parameters affect the vibration response.

Torsional vibratory modes are especially difficult to estimate, as damping predictions in the design phase are often based on reference and experience. Moreover, unlike for lateral modes, often no dedicated sensor is installed on a machine; as a



consequence these often go undetected. However in geared trains it is possible to identify torsional dynamics by observing proximity probe data, due to the gear mesh torsional-lateral coupling.

Sometimes it is possible to perform basic estimation of torsional damping by evaluating the vibration decay when the machine starts, trips, or in case of a sudden change in operating conditions. However such assessments are only possible for specific operating conditions and may fail to identify issues if the overall damping is not constant throughout the operating range, as for example in such cases as:

- Machines equipped with gearbox running on hydrodynamic bearings, where the damping depends on the oil film dynamic characteristics
- Grid connected machines (motors, generators), where damping from electromagnetic coupling may change with load as well as being influenced by electrical grid stability
- Machines with special couplings, e.g. variable speed couplings or polymeric couplings, with material damping dependent on operational parameters, e.g. load
- VSD motors, where the torsional dynamic becomes a function of the drive control loop settings (also applies for generators AVR settings).

Traditional experimental modal testing techniques rely on controlled and measured excitation together with measured responses in order to identify the mode shape, natural frequency and damping factor of each mode. Such assessments are in practice very difficult to obtain in actual operating conditions, principally due to the challenges of quantifying the excitation force.

Operational modal analysis (OMA) identifies the modal parameters of a system from measurement of response to unmeasured or unknown excitation. OMA has proven successful over the past several decades on non-rotating structures and has in the past years rose in prominence in the rotordynamic community.

Through examples based on various measurement and case studies, this paper will show and demonstrate how OMA can be used to:

- Successfully identify the damping of not only the fundamental torsional mode but also higher order torsional modes.
- Validate design models by tracking torsional damping variations depending on operating conditions.
- Aid operators and OEMs for machine tuning during commissioning.
- Provide an essential tool for troubleshooting

## INTRODUCTION

The correct estimation of torsional modal parameters, e.g. natural frequencies and damping, is of great importance in turbomachinery applications, beginning from the design phase to commissioning and operation. Excitation of a torsional vibration mode can cause severe torsional stresses and severe

damage to the equipment, often without any pre-emptive sign.

This is because usually no dedicated instruments are installed to detect this kind of vibratory mode, so there is little chance to tell whether the machine is experiencing excessive torsional stress.

Avoiding such problems starts by designing a rotor train where the frequencies of excitation sources and natural modes are reasonably separated. In operating conditions, the excitation of torsional vibrations may come from many sources which may or may not be a function of running speed, e.g. aerodynamic excitations, misalignments, etc.

So, for an optimal design with respect to system's dynamic response, one would need accurate information regarding excitation forces and system internal dynamics.

Excitation forces are usually known with sufficient degree of details from design considerations. Common excitation sources include once per revolution 1X (e.g. misalignment, coupling unbalance) and to a lesser degree 2X (misalignment). Additionally to these, specific system components are usually present and also generate excitation. In general, these sources include the system driver, such as a motor or turbine including their specific driving and control systems; and load, such as impellers, propellers, etc. Additionally, all gear meshes are excitation sources, see Eshelman, (1977) or Wachel and Szenasi (1993).

As for the system internal dynamics, whether simplified lumped parameter models or full finite element calculations are used, designers are today able to make relatively accurate predictions of the system's undamped natural frequencies and mode shapes, Wachel and Szenasi (1993).

In certain cases it is not possible to avoid operating a machine in conditions where an excitation source might interfere with a torsional resonance. In these cases it becomes of paramount importance to have an accurate estimate of the damping. The damping value affects the amplitude of the response to a harmonic excitation; secondly it affects the fatigue life estimation by affecting the rate of decay of torsional oscillations when external excitations are removed.

A damped analysis presents however an additional challenge, in that the system's damping needs to be estimated before a model can be setup and used to make predictions regarding e.g. forced and transient response, fatigue evaluation. Although a comprehensive discussion of torsional damping sources is outside the scope of this paper, one can broadly classify it in two categories, either external (associated to driving or driven forces/losses, or support forces) or internal (material hysteresis, internal frictions, etc.).

Within this framework, particular focus is given to geared turbomachinery trains, where supporting elements (journal bearings) couple the lateral and torsional dynamic of the train and thereby become the dominant source of torsional damping.

Generally, torsional damping for turbomachinery is very low in comparison to that of lateral vibrations because significant damping for the latter is obtained through radial motion in journal bearings that compresses the oil film, while in



torsional vibrations there is no radial motion associated to the vibration. That is, except for geared trains where the transmitted power and torsional vibrations are transmitted to radial (as well as thrust) static and dynamic forces through the gear mesh.

Predictions of torsional natural frequencies are generally thought to be accurate to  $\pm 5\%$  but examples of differences between predictions and measured results of up to 12% are given in Wang et al (2012). Validation of models and investigation of improvements is therefore of interest, Carden and Lindblad (2014).

Torsional modes may be identified by run-ups and -downs through the speed range. However, this results in identification only at a certain speed and particular operational conditions. Load conditions can affect the stiffness of couplings; an example is shown in Wang et al (2012), where the torsional natural frequency shifts by approximately 3% with changes in load. Furthermore phenomena exist whereby the torsional modes at stand still or off-load differ to those when the rotor train is in operation. Two examples are given in Carden and Lindblad (2014) where both measured natural frequencies and damping ratios showed very large discrepancies compared to the predictions.

Modal testing of rotordynamic systems can be undertaken for validation of dynamic behavior, updating and improvement of models and during troubleshooting and failure investigations. Traditional experimental modal testing techniques rely on controlled and measured excitation together with measured responses in order to identify the mode shape, natural frequency and damping factor of each mode. Applying a controlled and measured excitation to a rotor train when in operation is logistically difficult and especially challenging in intrinsically safe offshore environments typically encountered in the oil and gas industry, Carden et al. (2014).

Traditional Experimental Modal Analysis (EMA) can be used to measure the modal properties to facilitate the understanding of the dynamics of the systems, validate design models and assess operational health. These assessments are in practice cumbersome for a machine in operation.

Operational modal analysis (OMA) can identify the modal parameters of a system over its entire operational range from measurement of response due to some (unknown) excitation, Peeters and De Roeck (1999). Its advantage over EMA is that no controlled and measured exogenous excitation is required. The disadvantage of OMA is that scaling of the modal responses is not possible due to the amplitude of the excitation not being known.

OMA has proven successful on non-rotating structures, to the non-rotating structures of full scale machinery in the field, Clarke et al. (2011), Carden (2013), and more recently been applied to rotordynamic modal analysis, Carden et al. (2014), Carden and Lindblad (2014), Carden and Morosi (2014), Guglielmo et al. (2014).

## OMA BACKGROUND AND THEORETICAL BRIEF

Operational modal analysis has existed since the 80's with application mostly on large civil-engineering structures. A comprehensive literature overview has been presented by Purup (2014) and summarized hereby.

One of the first applications of OMA has been documented by Rubin (1981), where an offshore platform is investigated purely on the background of the ambient excitations of the waves. The method was systematized the first time in Felber (1993), who used the simple method of peak-picking. This simple method is widely used for EMA as well. The method simply involves creating a Power Spectral Density (PSD) plot on the basis of the ambient excitations and the peaks of the plot are then manually identified as the eigenfrequencies.

First, to give an overview of the modal analysis field a short introduction is made to classical EMA, the various OMA methods and the combined stochastic-deterministic method called Operational Modal Analysis with eXogenous Inputs (OMAX). Figure 1 gives an overview of the methods, Purup (2014).

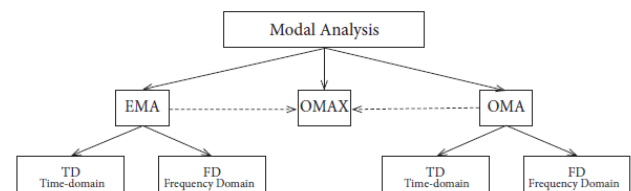


**Figure 1 - Overview of the modal analysis methods available**

**EMA.** These methods are deterministic methods, where a known input is used to excite the structure and the resulting response is measured as either acceleration or velocity in a number of nodes on the structure. These methods often require the structure to be taken out of its operating condition and into the laboratory to conduct the experiments. The structure will then be excited with either a hammer to create an impulse force or the structure will be subjected to a sinusoidal vibration from a shaker. The measured response will then be pre-processed and fed into an analysis algorithm and the dynamic properties can be identified.

**OMA.** For some structures the use of EMA is very inconvenient, if not impossible, to use. This is the case for many rotating machines, as well as many fixed structures, which are difficult to excite with a controlled force in operation. For these examples on-site measurements will be the only option and for this, OMA would be the easiest method.

Since the first researchers started working with OMA many algorithms have been developed. A selected literature review is presented in Table 1, Purup (2014).

Frequency domain methods exist, however in this paper further details are given to the time domain Stochastic Subspace Identification (SSI) methodology class. SSI techniques are considered to be among the most powerful class of the known identification techniques for natural input modal



analysis.

Frequency Domain Methods	
Method	Further info in
Peak-Picking	Rubin (1981)
Frequency Domain Decomposition	Brincker et al (2000), Brincker and Andersen (2001), Zhang et al. (2010)
Output-only Least Square Complex Frequency Domain	Zhang et al. (2005)
Time Domain Methods	
Natural Excitation Technique	James et al. (2006)
Data-driven Stochastic Subspace Identification	Peeters and De Roeck (1999)
Covariance-driven Stochastic Subspace Identification	Peeters and De Roeck (1999)
ARMAV	Ljung (1999)

**Table 1 – Selected literature review of OMA methods**

### The Stochastic Subspace Identification

Mathematically, structural systems may be recast from continuous second order differential equations governing their behavior into discrete state space equations. Stochastic Subspace Identification is an efficient method for identifying the state space matrices from measured response data, Carden and Lindblad (2014). The natural frequencies, damping parameters and mode shapes may then be extracted from these state space matrices. The major advantages of taking this approach are that it is quick and non-iterative and therefore does not suffer from convergence problems. Fundamental proofs and discussions of numerical stability are described in Van Overschee and De Moor (1996), while a succinct, though thorough, step-by-step procedure with an example application is provided in Peeters and De Roeck (1999).

There are various subtypes of SSI available: covariance-driven and data-driven SSI. The main difference between the algorithms is found in the data-reduction steps in the beginning of the algorithms.

The following mathematical brief provides a summary of the core of the SSI method, and it is adapted from and described in Carden et al. (2014).

The covariance-driven method starts off by forming a Toeplitz matrix holding covariances of a data Hankel matrix. This is fast, but comes at the cost of a less numerically stable algorithm. Another disadvantage of the covariance-driven method is the need for infinite measurements to satisfy the assumptions for the covariance function.

The data-driven approach generates a data Hankel matrix and uses QR-factorization to project the row space of the future outputs into the row space of the past reference outputs. A significant data-reduction is hereby achieved, but it is at the cost of computational time.

The core of data-driven SSI consists with the estimation of an extended observability matrix  $O_n$  in order to lay the basis of the estimation of the system state-space matrices  $A$  and  $C$ , see Overschee and De Moor (1996) for further details.

So to find  $O_n$  a weighted Hankel matrix  $\Gamma_n$  is built. The first task is to determine its dimension, by using the Singular Value Decomposition. The observability matrix is pre- and post-multiplied by weight matrices  $W_1$  and  $W_2$ , which are user-defined. Now taking the SVD of the resulting product yields:

$$\Gamma_n = W_1 O_n W_2 = USV^T$$

$$= (U_1 \quad U_2) \begin{pmatrix} S_1 & 0 \\ 0 & S_2 \end{pmatrix} \begin{pmatrix} V_1^T \\ V_2^T \end{pmatrix} \rightarrow U_1 S_1 V_1^T \quad (1)$$

In theory the number of non-zero singular values will equal the order of the system,  $n$ . In Eqn. (1) the singular value matrix is broken into  $S_1$  and  $S_2$ . As noted by Carden et al (2014), with perfect numerical accuracy and absolutely clean data,  $S_1$  would be comprised of a diagonal of  $n$  non-zero entries and  $S_2$  would be comprised of all zeros. In practice however this seldom happens and it is up to the analyst's skill and experience to choose the correct order. Once an order is chosen, the extended observability matrix may be calculated as shown in Eqn. (2).

$$O_i = U_1 S_1^{1/2} \quad (2)$$

The only significant difference between the different stochastic subspace methods is the choice of the weight matrices  $W_1$  and  $W_2$ .

Three different algorithms are often used in the SSI techniques, the Un-weighted Principal Component (UPC), the Principal Component (PC) and the Canonical Variate Analysis (CVA) algorithms. As a practical rule, UPC is a good choice in the presence of modes of equal strength and data with good signal-to-noise ratio. CVA performs well with noisy data and modes characterized by widely different strength. PC can be considered as a compromise between UPC and CVA. Nevertheless, it should be remarked that in practice the algorithms have shown to perform similarly in a multitude of field testing, as also investigated and reported in Zhang et al. (2005).

The dynamic matrix  $A$  may be calculated in a least squares manner by making use of the shift structure of the observability matrix as shown in Eqn. (3). The eigenvalues of this dynamic matrix  $\lambda_d$  are the poles of the system in discrete time and are converted to continuous time using Eqn. (4).

$$A = \underline{O_n}^\dagger \overline{O_n} \quad (3)$$



$$\lambda_c = \frac{\ln(\lambda_d)}{\Delta t} \quad (4)$$

The natural frequency and damping are then extracted from Eqn (4). Mode shapes may also be extracted from the eigenvectors, see Peeters and De Roeck (1999) for details.

OMA essentially assumes that the excitation is white. In presence of colored excitation, spurious “noise” modes are extracted as well, which correspond to the poles of the theoretical transfer function which would convert white noise to the colored. Additionally, when the system is over-determined then poles related to noise and numerical errors will be present, Carden and Lindblad (2014).

### OMA Stability Diagrams

Often identifying what is a real mode from noise relies on the judgment of the analyst. This process has been eased by the introduction of the concept of stability, Van der Auweraer and Peeters (2004).

The stability diagram is formed by choosing a range of values for  $n$ , the order of the system, and extracting the modal parameters from the dynamic matrix for each of these values Van der Auweraer and Peeters (2004). An example of a stability diagram is shown in Figure 2.

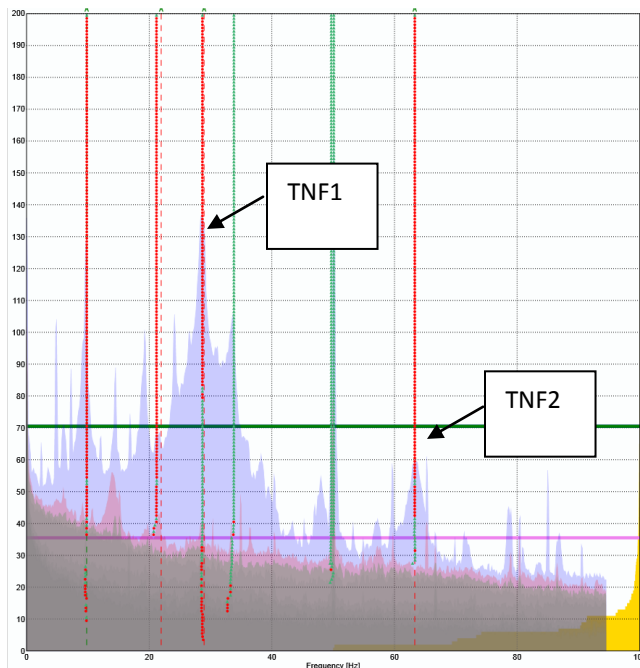


**Figure 2 – Example of OMA stabilization diagram for Case study 1.**

The mean power spectral density of the radial proximity probes on a compressor gearbox is under laid on the figure. A column of poles that pass the rules such as those stated above are a strong indicator of a potential mode and are indicated by red dots in Figure 2. Note that other possible modes are

identified, but not all are necessarily associated with (torsional) modes. Poles that change value significantly as the order is increased are typically related to noise and numerical round off errors, green dots. This classification is again relying on the judgment of the analyst and criteria often depend on the type of system that is being analyzed. Typically, selection criteria include limiting the variations of natural frequency, damping and modal assurance criterion.

Further discussion of Figure 2 is given during the presentation of more detailed results.

### Assumptions of the SSI method

When deriving the algorithm for SSI it is necessary to make a number of assumptions, some of which are difficult to fulfill in practical measurements, Peeters and De Roeck (1999) and Purup (2014):

1. Sensor inaccuracy and modeling inaccuracies are modelled as white gaussian noise with zero mean.
2. The noise terms will have a zero mean
3. Stationary stochastic process: State covariance is assumed to be independent of time
4. Noise terms are independent of the actual state
5. All modes are excited by stochastic input.

The first assumption refers to the contribution of the measured signals of non-measurable vector signals assumed to white noised and a given covariance matrices. In addition to the modes, the identified system may contain poles associated with features of the data acquisition chain such as the poles of an anti-alias filter, Carden and Lindblad (2014).

The second assumption is practically taken care of by removing the mean of the measured data.

When performing measurements on an actual machine one should be aware of the third assumption that the process should be time-independent. It should be noted that the SSI algorithms in Van Overschee and De Moor (1996) and Peeters and De Roeck (1999) are based on the dynamic response properties of the system being stationary. Therefore when applied to rotating machinery for the identification of torsional modes which depend on the operating conditions, the data must be used during a period when the machine is operated at a stable speed and set of process conditions.

Assuming that noise terms are independent of the state of the system is true in most situations. It is hard to think of a situation where the noise from sensors would vary with the state of the system.

Finally, the assumption that all modes should be excited by stochastic input often does not formally hold in practical situations. Typical violation of this assumption are related to e.g. colored excitation such as harmonics of the running speeds of the machinery, orders of the firing rate of an engine, flow related phenomena etc. Carden and Lindblad (2014). It is then clear that this is definitely violated when the algorithm is applied to rotating machinery, where the input contains some dominant (harmonic) frequency components. The implication is

that some dominant frequencies will appear in the stability diagram. Although several methods have been devised in order to deal with harmonic excitation, see Peeters et al. (2013), a practical rule of thumb is that poles associated with harmonics have zero or close to zero damping.

If not careful, ignoring these assumptions has the consequence that modes could be wrongly classified and/or overlooked. Again, it is down to the analyst to form an opinion on the result based on the expected dynamic properties of the structure.

### Influence of Damping

Unless the modes are closely spaced, estimating the natural frequencies of a structure is done with acceptable precision just creating a simple PSD plot. Where the OMA method really adds value is therefore when damping parameters also can be determined, Purup (2014). When damping is introduced, the undamped natural frequencies will change to be damped natural frequencies with the well-known relationship:

$$f_d = f_0 \sqrt{1 - \zeta^2} \quad (7)$$

When identifying natural frequencies experimentally, the damped natural frequencies will always be identified.

In most cases the influence of damping on the size of the damped natural frequency will be negligible, Eqn. (7), and it can therefore be assumed that  $f_d = f_0$ .

Purup (2014) performed numerous numerical and experimental verifications of the damping estimated using SSI algorithms, on both fixed structures and rotating shafts. The results indicate that the OMA provides slight overestimations of the damping when calculating the lateral modes. This is especially observed for the high damped systems. This has been identified as a problem for OMA algorithms before, e.g. by Avitabile (2002).

### TORSIONAL LATERAL COUPLING

For lateral vibrations the main source of damping is the bearings. For torsional systems without a gear, there are normally no other sources of damping than the material damping in shafts and in the couplings.

In a torsional natural frequency analysis this damping is normally disregarded, as the limited damping does not alter the natural frequencies.

When the rotor train includes a gear, there is a coupling to the lateral response via the tooth engagement which allows for transfer of energy (including dissipation) between lateral and torsional degrees of freedom.

How much dissipation the gear element introduces in the coupled system is then strongly associated to the contribution associated with the bearing dynamic coefficients.

Turbomachinery gearboxes are usually supported by hydrodynamic bearings. In this type of bearings the lateral motion squeezes the oil in journal bearings, thus introducing a

damping effect that increases the total damping in the system.

It is well known that their hydrodynamic stiffness and damping coefficients depend on a number of design and operational parameters; see for example Hamrock, (1994).

Variation of these parameters will then have an influence on the torsional dynamic properties of the system.

When considering operating conditions of a typical turbomachine, one typically concentrates on the operational parameters, such as speed and oil inlet temperature (viscosity) variations. In gearboxes another operating parameter that significantly influences the bearings dynamic coefficients is the tangential load, as it acts and effective pre-load force on the bearing.

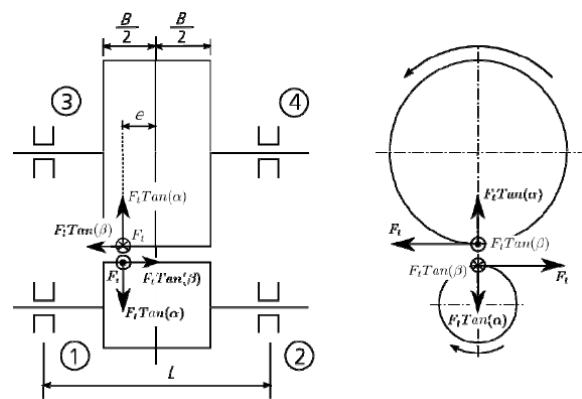


Figure 3 – Diagram of transmitted forces in parallel shaft gearbox.  $F_t$  is the tangential contact force.



**CASE STUDIES**

**CASE STUDY 1: ELECTRIC DRIVEN CENTRIFUGAL COMPRESSOR**

The first case study regards a 40+ MW centrifugal compressor train, driven by a variable frequency (LCI type) synchronous motor via a speed increasing gearbox. The outline of the system is shown in Figure 4.

The results shown hereby include the main findings recorded during the commissioning of the unit, during which full Level 1 performance testing was performed.

The main purpose of this case study is to illustrate how the prediction of torsional dynamic performance of a geared train can be verified during commissioning by using OMA parameter identification techniques.

Moreover, it will be shown how OMA can help with a quick identification of the origin of subsynchronous frequency components which appeared during testing, ultimately expediting the commissioning process.

**Baseline numerical predictions**

Firstly, the numerical predictions of the torsional dynamic analysis are hereby presented.

The analysis has been performed by use of the dynamic finite element code RP, developed by LRC.

Shaft elements have been modeled using an Euler beam formulation. The stiffness of the shaft couplings are represented by simple torsional springs with spring rates according to the drawings. The gear ratio and tooth flexibility is included by means of a special gear finite element.



**Figure 4 – Outline of the torsional dynamic system. From left to right: compressor, pinion gear (lower center), wheel gear (upper center), electric motor (right).**

The calculated lowest natural frequencies are found in Table 2. The corresponding mode shapes are found in Figure 5. The torsional Campbell diagram is presented in Figure 6.

Mode	Frequency [Hz]
1	27.5
2	62.8
3	137.9
4	253.2
5	300.9

**Table 2 – Predicted first 5 torsional frequencies**

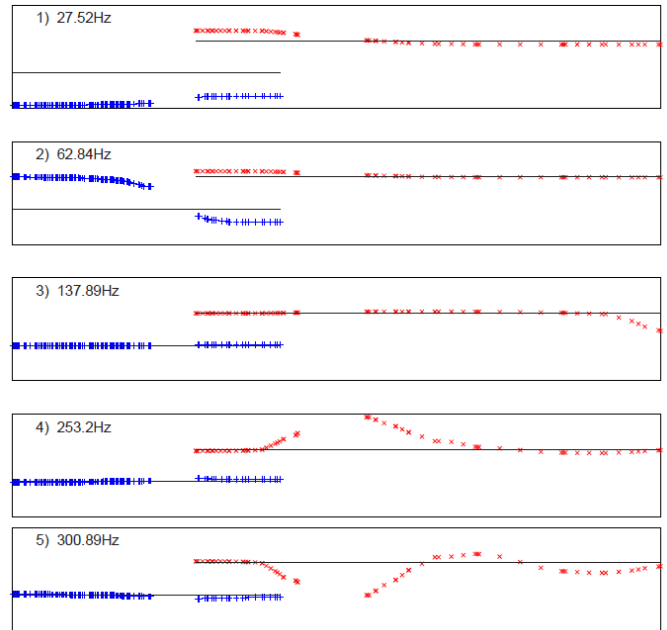


**Figure 5 - Predicted first 5 torsional mode shapes**

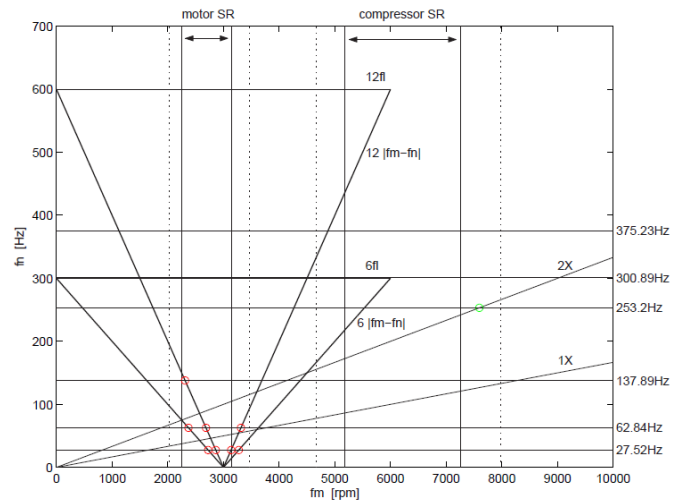


**Figure 6 – Torsional Campbell diagram**

**Measurements**

Measurements have been obtained during the machine dynamic testing while in the commissioning phase. Compressor dynamic testing is a technique of establishing equipment operating profiles by running the equipment through a series of structured tests. It is conducted to confirm that the equipment will perform under field conditions to vendor’s specifications and also to confirm the results of factory acceptance tests.

The objective for the performed test on this machine was that the operator wanted to avoid issues incurred with similar equipment installed at the plant.

The core of the performance test is to perform a verification of the compressor performance map. This means



running the machine at specific operating points, varying operating speed, inlet and discharge process parameters. A series of points have been recorded for the test, as shown in Figure 7, where a typical compressor performance map (head vs. flow) is shown. Note that green lines are iso-speed, at 75%, 80%, 95% and 100% of the nominal speed. Each number along these lines represents a performance point. The compressor has been tested at each point in steady condition, e.g. allowing all transients to decay.

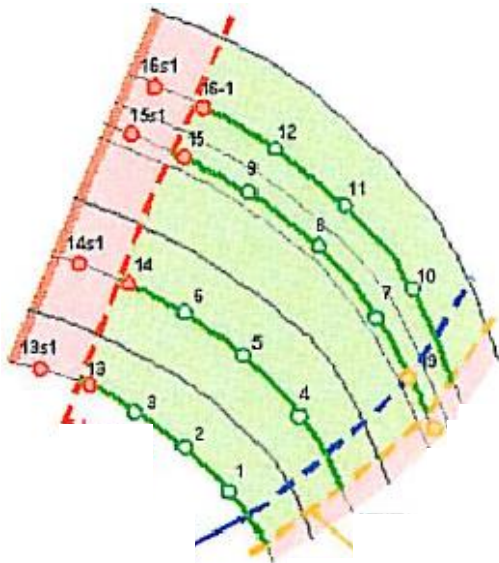


**Figure 7 – Compressor performance map. Gas flow (abscissa) and compressor head (ordinate).**

### Model identification using OMA

OMA analysis has been performed on the measurements relative to each of these points. The length of the time interval for each analysis is 10 minutes. This is longer than normally required, however longer measurements allow for more consistent results; it is always recommended to use longer than necessary time sequences if these are available.

Shaft vibration signals were taken directly from the Bentley Nevada acquisition unit installed on site.

A total of 8 radial proximity probe data have been used for the OMA analysis, 2 for each pinion and bull gear shafts Drive End (DE) and Non-Drive End (NDE) proximity probes.

As part of the dynamic evaluation, results have also been compared to torque data measured by a dedicated torque meter installed and integral part of the low speed side coupling, between motor and gear.

The results of the analysis are summarized in Table 3. For each test point, the operational conditions are specified, e.g. speed and load (torque). OMA has been used to identify the 1<sup>st</sup> and 2<sup>nd</sup> Torsional Natural Frequencies (TNFs) and the relative damping ratios.

For the first natural mode, TNF1, estimates have been made by analyzing both proximity probe data and torque meter

data, with very good agreement between the two. For second natural mode, TNF2, only proximity data analysis was possible, due to the too limited bandwidth of the torque meter.

As preliminary general considerations one can notice how OMA predicted natural frequencies are in good agreement with the theoretical values presented in Table 1. As for the damping ratios, it is also noted how the range is consistent to traditional assumptions for geared trains, where 1%-2% values are often used.

In Figure 8, the OMA results are presented for TNF1, frequency and damping, as function of the applied load. It is observed that the value of the natural frequency remains substantially constant irrespectively of the applied load. A very modest increasing trend may be noticed, especially in the torque meter estimation.

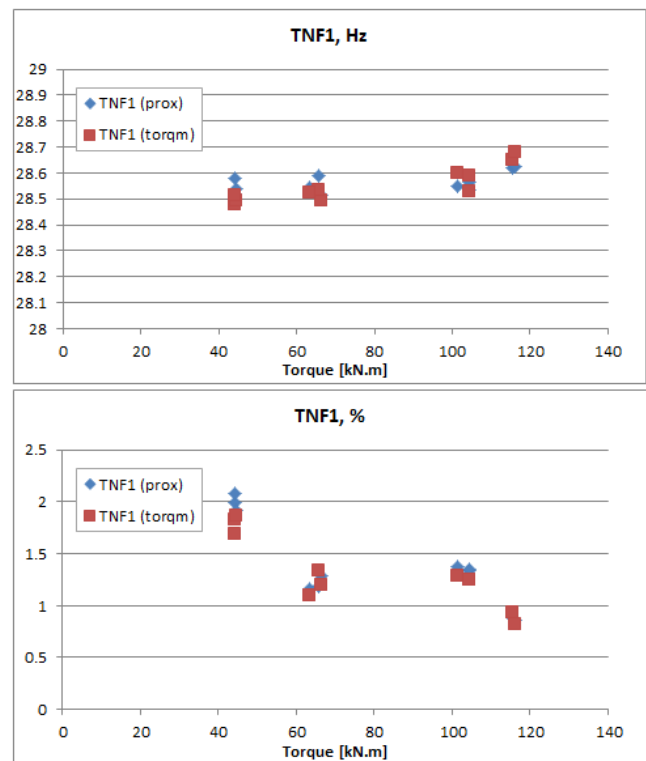


**Figure 8 – Trend of OMA for TNF1, proxy probe and torque meter data.**

As for the damping, the general trend shows how this parameter is decreasing as function of the load.

The behavior of frequency and damping as function of varying operating conditions can be related to different reasons, among which: the combined hydrodynamic stiffness and damping variations from the oil film in the gearbox bearings due to load and speed variations; variations of electromagnetic dynamic coupling from the motor at different load; VSD motor active control. This falls outside the scope of this analysis and is not further discussed in this framework.

Note that for test points 7-9, at a compressor speed 6642





rpm, the damping has been estimated using an OMA frequency domain method, Frequency Domain Decomposition. This is because at that speed there is a torsional interharmonic frequency from the LCI drive which coincides with and excites TNF1. Although SSI algorithms could identify correctly the natural frequency value, a reliable damping estimate was not possible. For this reason an OMA frequency domain method, Frequency Domain Decomposition (FDD) was employed, which provided a more reliable estimation in presence of harmonics, although not fully satisfactory. This considerations just add to what discussed above regarding the inherent difficult of performing OMA estimation when the selected mode is coincident or very close to a harmonic frequency excitation components.

Similarly to TNF1, see Figure 9, the OMA results are presented for TNF2, frequency and damping, as function of the applied load. Also in this case the frequency values are constant with respect of the applied load. However it is noted how the damping values are not significantly affected by the load; the overall trend is decreasing as for the first mode, but the dependency appears weaker.

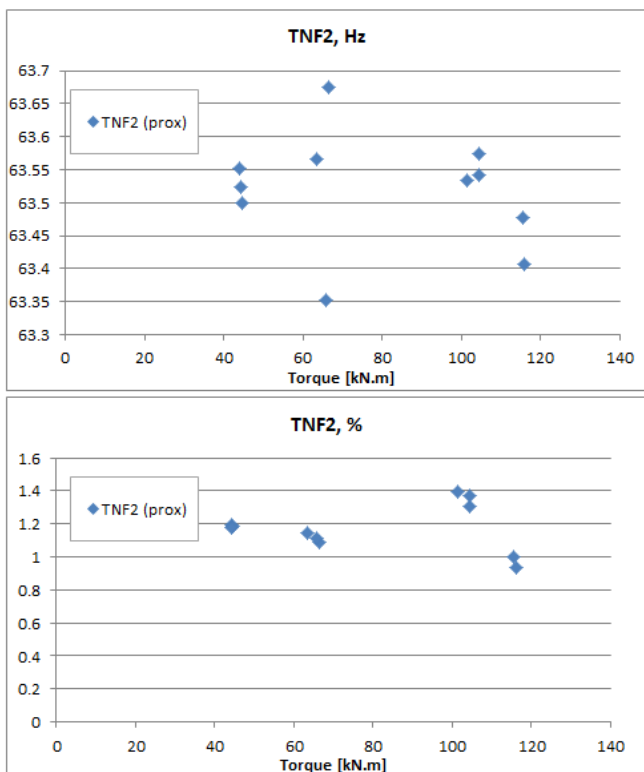


Figure 9 - Trend of OMA for TNF2, proxy probe data.

As already argued by Carden and Lindblad (2014), OMA results have variances, just like EMA. In practical terms the identification of the modal parameters from several sets of data will provide confidence in the results as it is statistically unlikely to identify a group of results all lying in an extreme fringe of a distribution. For the present case study, 8 channels were considered simultaneously, with time block-sets of 10 minutes; typical standard deviations of the SSI estimate on the e.g. first natural frequency were observed in the order of 0.05-0.30 Hz and 0.01-0.15% for the damping; note the ranges are given as standard deviation differ slightly depending on the test point considered. This approach is demonstrated in this case study where the consistency of the torsional mode natural frequency and damping at different loads provided confidence in the precision of the identification.

It is the author's experience with typical rotor systems that a few minutes of data at steady speed and operational conditions give a reliable result with low variance. More formally, one can take the natural frequency estimation as an example; as discussed in Carden and Morosi (2014), the OMA estimates will be close to having a Gaussian distribution and therefore there is approximately 95 % confidence that a single identified natural frequency would be within  $\pm 2 \times 0.30 \text{ Hz} = \pm 0.60 \text{ Hz}$  of that identified (for the worst case test point identified, with reference to the 0.05-0.30 Hz range presented above). Although this is a reasonable result in itself, in a continuous monitoring context the judgment would be made on the mean of a series of results and the standard deviation of the mean is  $1/N^{1/2}$  where N is the number of estimates of the parameters used to calculate the mean. Thus the confidence band on the identified result will be far narrower than  $\pm 0.60 \text{ Hz}$  and dependent on the length of time of operation.

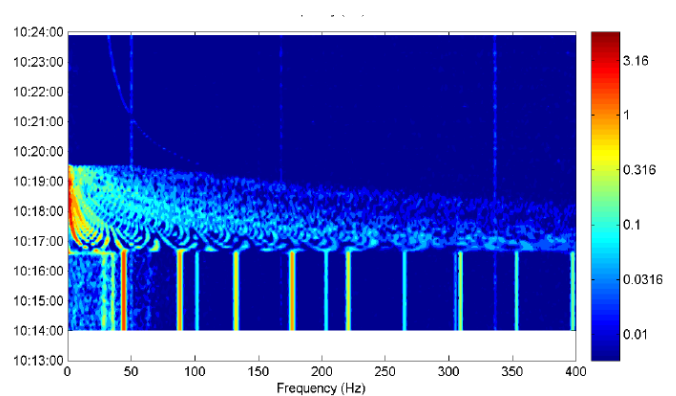


Figure 10 – Contour plot of vibration levels during trip, gearbox wheel DE x probe. Time upwards; frequency from left to right



Test point #	Speed rpm	Torque kN.m	TNF1 (prox probes)		TNF1 (torquemeter)		TNF2 (prox probes)	
			Hz	%	Hz	%	Hz	%
1	5216	44.3	28.5	1.99	28.5	1.82	63.5	1.19
2	5216	44.5	28.5	1.91	28.5	1.87	63.5	1.19
3	5216	44.1	28.6	2.08	28.5	1.79	63.5	1.18
4	5897	66.5	28.5	1.28	28.5	1.20	63.7	1.09
5	5898	65.7	28.6	1.18	28.5	1.13	63.3	1.12
6	5898	63.4	28.5	1.16	28.5	1.10	63.6	1.14
7*	6642	104.3	28.6	1.33	28.6	1.25	63.6	1.30
8*	6644	104.3	28.5	1.35	28.5	1.25	63.5	1.37
9*	6644	101.5	28.5	1.37	28.6	1.29	63.5	1.39
10	6923	115.5	28.6	0.88	28.6	0.93	63.5	1.00
11	6925	116.0	28.6	0.86	28.7	0.81	63.4	0.93

**Table 3- OMA summary results. Note that the asterisk \* indicates that the mode has been estimated using an OMA frequency domain method, Frequency Domain Decomposition.**

### Comparison with traditional identification methods

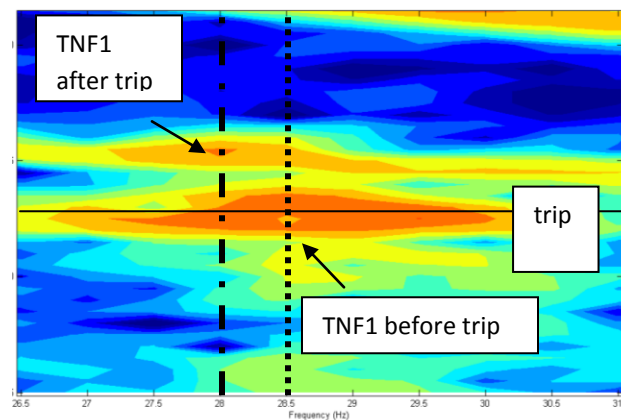
Damping values obtained with OMA have been compared to those identified by traditional means, e.g. without using OMA.

Figure 10 shows the spectrogram of the gear wheel during a trip. Firstly, it should be noted that torsional natural frequency appears to shift slightly after the trip. This is noticeable looking at Figure 11, where a detail of the same plot of Figure 10 is presented. The shift is approximately 0.5 Hz, from 28.5 Hz to 28.0 Hz. This shift indicates a difference in the torsional dynamic behavior of the train when on and off load. It is considered that the shift was probably caused by the added stiffness due to the magnetic flux within the motor present when on load. A similar behavior has been observed also by Carden and Lindblad (2014), though this was not calculated nor further quantified numerically within the project.

The damping was estimated on the basis of the free fluctuation. Estimation has been accomplished by fitting a single degree of freedom harmonic oscillation with damping to the band pass filtered vibration decay, see Figure 12. The issue of estimating the damping during a trip (or even a step response) is that a sudden load changes on the gearbox causes large displacement amplitudes in the bearings, see Figure 13 —, therefore noticeably affecting their dynamic coefficients, including the damping, which appear not constant in time. This leads to issues with the correct identification of the damping. Moreover, as discussed earlier regarding the shift of natural frequency, during a trip the dynamic contribution to the damping due to electromagnetic torque in the motor is missing.

In a further attempt to estimate damping during operation, the amplification of TNF1 has been evaluated while excited by a sweep of torsional interharmonic frequency caused by the VSD operation as presented in the waterfall plot in Figure 14.

The amplification factor for the 1st torsional mode can be calculated to approximately  $Q = 1/2\xi = 30$  based on the values shown in Figure 14. This corresponds to a damping ratio of approx. 1.7% which is consistent, although slightly higher for that load (approx.. 60 kNm), to what observed with OMA analysis, see Table 3. A possible reason for higher damping is due to the length of the excitation frequency sweep, which if too low leads to underestimation of the amplification factor.



**Figure 11 – Detail of contour plot of vibration levels during trip, gearbox wheel DE x probe, showing the shift in natural frequency.**



### Conclusions for Case study 1

In this case study it has been shown how operational modal analysis can identify the modal parameters of a system over most of its typical operational range from measurements of response due to unmeasured excitation.

Parameter estimation obtained with proximity probe data proved to be as reliable as with dedicated torsional vibration recording equipment. This means that detailed torsional dynamics of geared turbomachinery can be evaluated with OMA algorithms with the sole use of readily available vibration data.

Acquiring such information during commissioning can be seen as a reference point for future surveys and better understanding of the root cause of deviations from the baseline behavior.

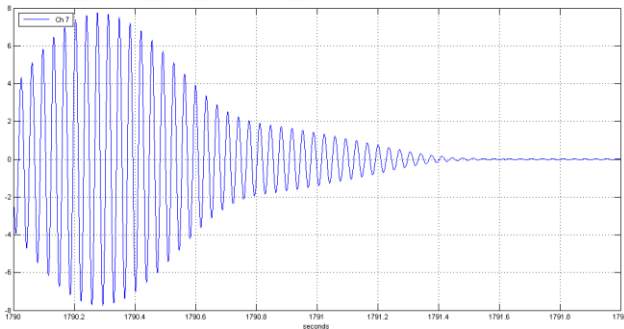


Figure 12 – Vibration decay of gearbox wheel DE x probe after a trip (band-pass filtered).

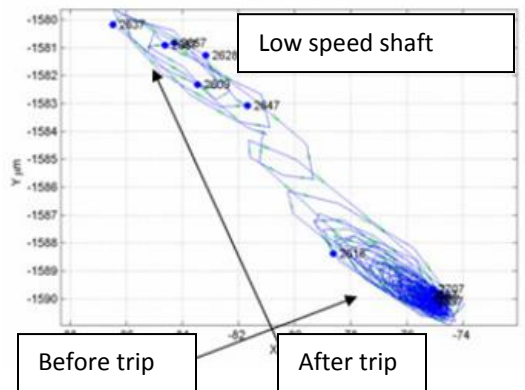


Figure 13 – Illustration of the gearbox wheel DE x and y probes centerline orbit during trip, showing large displacements.

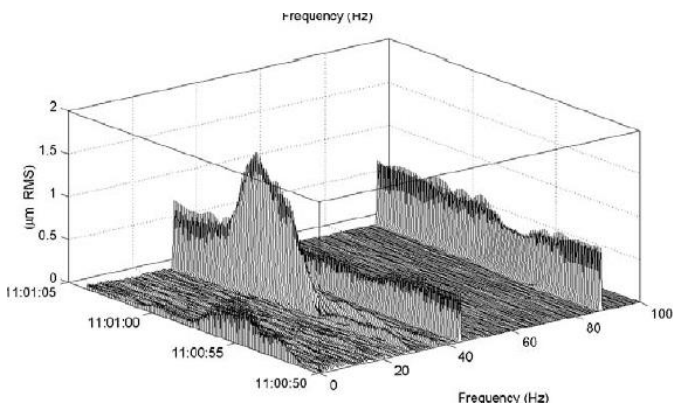


Figure 14 - Waterfall plot of gearbox wheel, NDE x probe



## CASE STUDY 2: GAS TURBINE DRIVEN GENERATOR ON BOARD OF FPSO

The results from the following case are obtained from measurements on one of three identical approx. 30 MW gas turbine driven generators, installed on an FPSO vessel. During FAT of the units, high sub-synchronous vibration amplitudes were experienced during low load operations. The frequency of the vibration component indicated a relation to the 1st torsional natural vibration mode of the rotor system, transforming to lateral vibration by the tooth engagement in the gearbox.

In order to evaluate the rotordynamic stability and fatigue conditions of the shafts, it was decided to experimentally determine the modal parameters of the first torsional modes that inherently show little damping. The parameters were then used for updating of a coupled torsional/lateral rotordynamic model for analysis of the problem.

The original approach for the modal analysis was applying a step load change to the generator, using a resistor load bank provided for the purpose. Later on, sequences with constant load have been used for OMA as alternative approach for determination of the torsional natural frequencies and damping parameters. Results from both methods are presented and discussed in the following.

### Gas turbine generator and test setup

The generator units consist each of a two shaft gas turbine driving an approx. 30 MW generator through a speed reducing gearbox, with gear ratio of approx. 1500/6200. The low-speed gear wheel rotor was designed with a concentric quill shaft arrangement.

All three units were on the FPSO operated in parallel and shared load as dictated by demand.

The measurements for extraction of the torsional modal parameters were taken on the unit that had shown the highest sub-synchronous vibration amplitudes during the FAT.

It was decided to use a step load change on the generator, in order to excite the torsional modes of the rotor system. The electrical current step load was established using a temporary resistor load bank that almost instantly could be coupled in and out with a variable amount of load. The power absorption capacity of the resistor bank was limited to 7.5 MW, which was sufficient because the vibration problem related to low load conditions.

The primary physical parameter used for extraction of the torsional modal parameters was the shaft torque, which was measured using strain-gauges, specially mounted for the purpose, on the low-speed coupling between the gearbox and generator. The signal was transmitted using RF telemetry.

The 'input' signal for the test was the motor current, which was measured using a current transformer fitted on a secondary lead from one of the three phases of the generator, in the dedicated switchboard room.

As supplement, the signals from the permanent shaft proximity probes of the gearbox, generator and gas-turbine was also captured.

All signals were during the test digitally recorded with high sampling rate for later analysis.

### Rotordynamic predictions

The dynamics of the combined rotor system was predicted using a coupled lateral/torsional rotordynamic model, using a Finite Element code. The model included a comprehensive formulation of the oil film bearing dynamic coefficients, as function of speed, load and temperature. For the combined torsional and lateral mode shapes, the primary dynamic losses are expected arising from the shaft movements in the oil film bearing of the gearbox, whereas the losses due to the oil film in the tooth engagement are evaluated less dominating.

The two lowest primarily torsional modes were predicted at approx. 15 Hz and 37 Hz. The predicted mode shapes of these two modes are shown in Figure 15 and Figure 16.

As indicated by the mode shape figures, the two torsional modes show a torsional gradient at the low-speed coupling, which is necessary for obtaining a proper strain / torque signal for the step response approach. The mode shapes show also significant lateral movements at the gearbox bearings, which complementary are necessary for the approach using OMA on the proximity probes, for extraction of the modal frequency and damping.

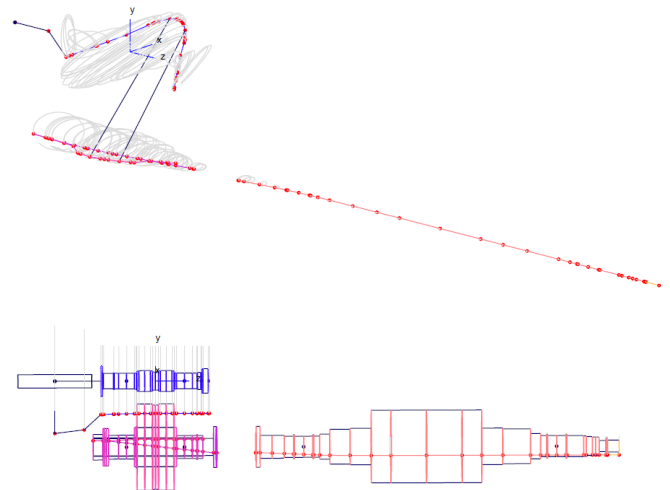


**Figure 15 - Predicted mode shape of the first torsional mode at approx. 15 Hz. The upper figure illustrates the lateral displacement orbits of the shafts. The lower figure illustrates the angular displacements of the shafts.**

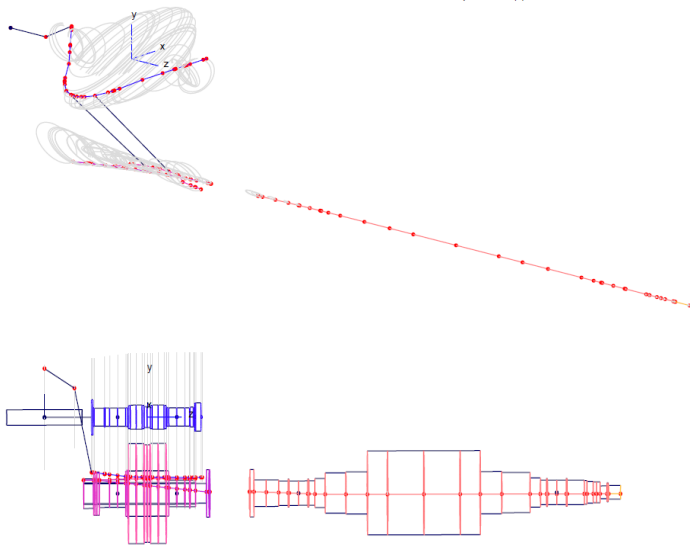


**Figure 16 - Predicted mode shape of the second torsional mode at approx. 37 Hz. The upper figure illustrates the lateral displacement orbits of the shafts. The lower figure illustrates the angular displacements of the shafts.**

**Modal properties from step responses**

The step response test was carried out on the generator unit after a run at constant loading for thermal stabilization of the unit.

During the actual test the step up- and off-loading was done in sequences of a couple of minutes as illustrated in Figure 17.

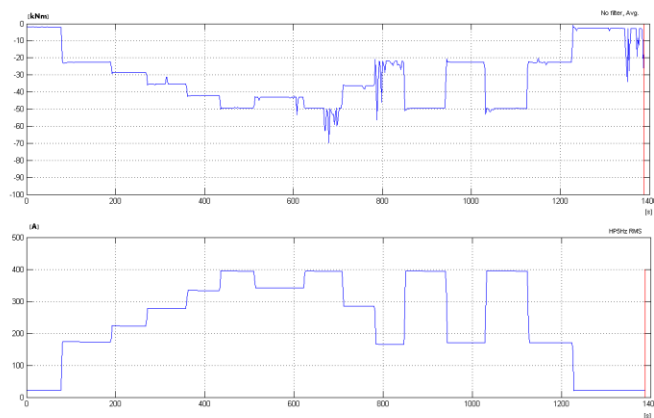


**Figure 17 - Electrical current from one phase of the generator (upper) and static shaft torque measured by the strain-gauge probe at the low-speed coupling (lower), during the test.**

In order to evaluate the modal responses and the signal-to-noise in the signals, the Frequency Response Function (FRF)

was extracted from the measurements. The signal processing for this, consisted in an enveloping of the harmonic current signal, using Hilbert transformation, followed by a differentiation by time of both the current envelope and the torque signals, as illustrated in Figure 18. From these two signals the FRF was composed as the example in Figure 19 shows. The FRF show clear indication of modal ‘peaks’ at the expected frequencies, but also some noise at the line frequency of 25 Hz.

For extraction of the modal frequency and damping, the torque response signal was band-pass filtered with appropriate band width, and then rectified. The decay slope relating to the modal damping was fitted using enveloping of the signal as illustrated in Figure 20. The natural frequency was determined by zero-cross counting on the processed signal.

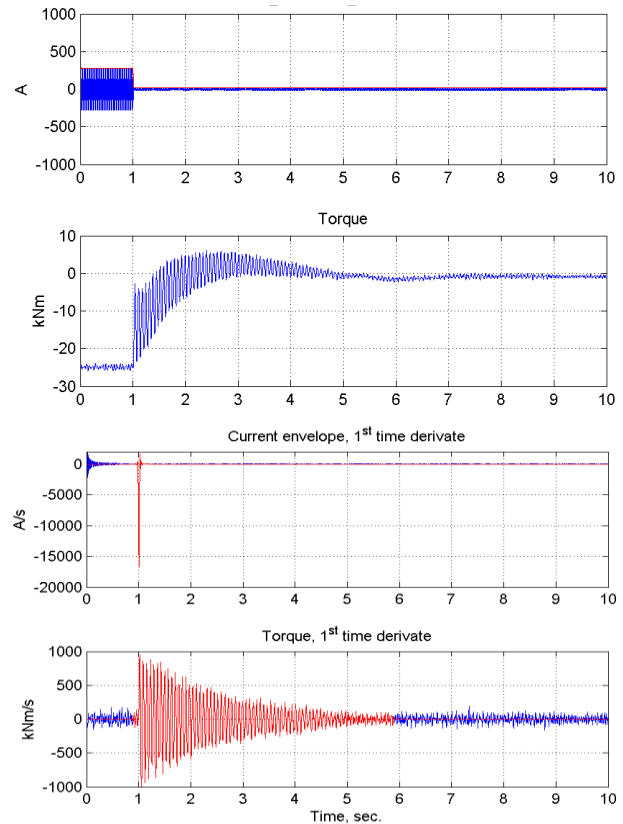


**Figure 18 - An example of a load step change from 14% to 0.7% rated power, showing the current for one generator phase with amplitude envelope (upper), the shaft torque response as measured by the strain-gauge at the low-speed coupling (2nd row) the 1st time derivate of the current envelope (3rd row) and of the torque signal (lower)**



For most load step changes not ending with a light load, the dynamic torque response showed a non-linear decay characteristic, with a reasonable decay at start followed by an abrupt disappearance of the dynamic torque, as illustrated in Figure 21. For these situations, the decay rate and thus the damping, was estimated from the first linear part of the dynamic torque response.

The reason for this behavior is probably due to the non-linear dynamics occurring during the load driven shaft relocation in the oil film bearings, caused by the eccentricity-dependent behavior for stiffness and damping coefficients of the bearing. This assumption is partly supported by the load dependency shown by the derived modal frequency and damping, illustrated in Figure 23. Also the transient dynamics of the electro-magnetic interactions in the generator might show non-linear contributions to the shaft torque.

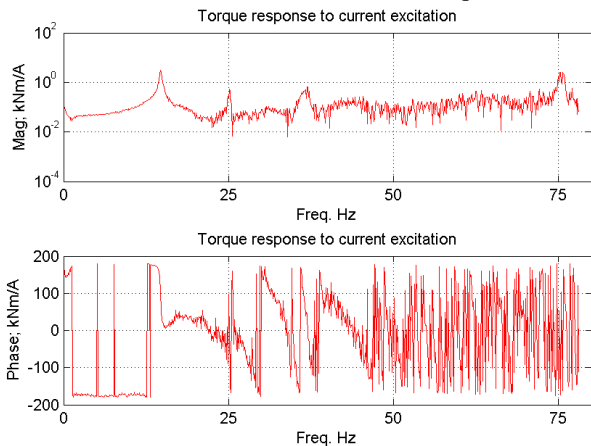


**Figure 19 - The Frequency Response Function derived from the current slope signal and the torque slope signal, shown in the two lower rows in Figure 18.**

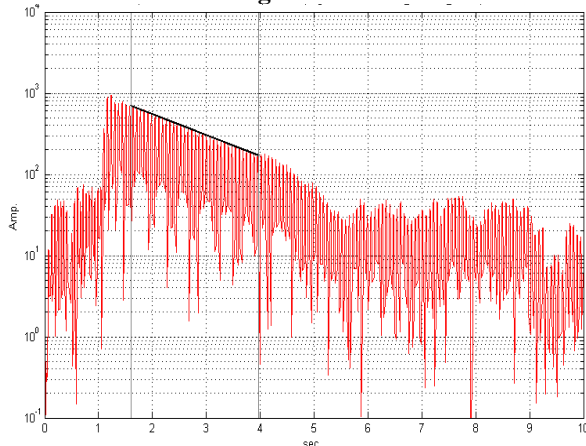


**Figure 20 - An example of the band-pass filtered and rectified torque time response signal, for extraction of modal frequency and damping. Note the logarithmic amplitude axis.**

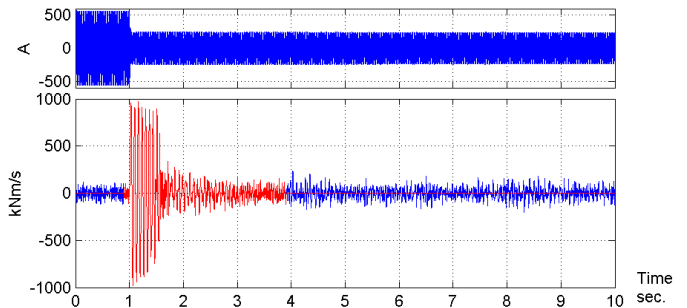


**Figure 21 - An example of a load step change from 26% to 11% rated power, showing non-linear behavior in the decay of the shaft torque response signal**

The modal frequencies and damping ratios extracted from a number of load changes, following the described method, are shown in Table 4. The load cases are expressed as the fraction of nominal power of the generator.

Case	% Rated Power	TNF1		TNF2	
		Hz	%	Hz	%
1.	11.4 → 1.4	14.7	0.57		
2.	13.2 → 1.4	14.8	0.65	37.2	0.41
<b>Avg.:</b>		<b>14.8</b>	<b>0.6</b>	<b>37.2</b>	<b>0.4</b>
3.	1.1 → 11.8	14.6	0.54		
4.	19.3 → 11.1	14.5	1.77		
<b>Avg.:</b>		<b>14.6</b>	<b>1.2</b>		
5.	1.1 → 26.8	15.3	3.69		
6.	22.5 → 26.4	14.8	0.74		
<b>Avg.:</b>		<b>15.1</b>	<b>2.2</b>		

**Table 4 - Modal frequencies and damping ratios (pct. of critical damping) extracted from the shaft torque response to a set of step load changes.**

As it appears from the table, it was only possible to estimate values for the 2nd torsional mode for the low load case, as the filtered torques step response showed no reliable decay for the higher load cases.

#### Modal properties from OMA

A number of signal sequences with the generator unit running at steady conditions have been extracted from the original measurements for OMA. Some of the sequences are taken as elongations from the signals used for the original step load analysis, but a few are taken at other instances with longer periods, which favor the OMA results. As a rule of thumb, the



signal used for OMA should extend at least 1000 periods of the mode with the lowest natural frequency of interest, i.e. in this case approx. 67 sec. for the first torsional mode at approx. 15 Hz.

For execution of the OMA the commercial available code Artemis was used together with some custom made Matlab tools for editing and evaluation of the signals. A number of OMA methods, counting both frequency and time domain methods, were used for the initial analysis. An example of the derived SVD spectra and stability diagram from the analysis is shown in Figure 22.

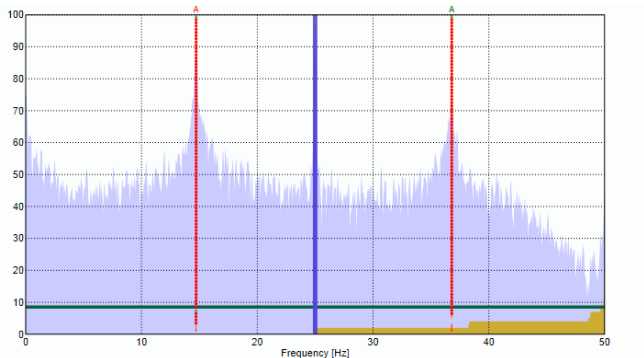


**Figure 22 - Example of derived SVD spectra and stability diagram from the analysis using the Stochastic Sub-space Identification - Principal Component (SSI-PC) method.**

The results from the OMA is in the following given for three different load conditions, expressed as the fraction of nominal power of the generator. All results presented are obtained using Stochastic Sub-space Identification methods on either the temporary shaft torque strain-gauges on the low-speed coupling, or on the 4 times 2 (X-Y) permanent proximity probes at the gearbox bearings.

The torsional modal frequencies and damping ratios extracted from the shaft torque strain-gauge signal are listed in Table 5, and the results extracted from the proximity probes are listed in Table 6.

For ease of comparison of the results, the data is plotted in Figure 23 where the data from the proximity probes are shown as averages from each load group.

The estimates from the three different approaches indicate a good correspondence regarding the modal frequencies and damping ratios, for the two lowest load cases, i.e. approx. 1% and 11% of rated power.

For the highest load case, approx. 27% of rated power, the estimates of both the modal frequency and damping seem to be significantly higher when using the step response method in relation to the OMA method. As indicated above and illustrated in Figure 21, the decay of the step responses showed some non-linear behavior in the cases where the load step ended with a certain amount of loading. This behavior was more pronounced

the high the end load was, influencing the certainty in the extraction of the decay rate from the response at the higher loadings.

As can be seen from the data in Table 6, some deviation appear between the results from the individual cases. This count especially for the damping estimates of the first torsional mode at 11% rated power, where values between 0.41% and 1.45% appear. The reason for this deviation is difficult to give as the individual numbers seem reasonable when studying the data, e.g. the deviation in mode 'peakiness' in the PSD spectra of the signals. This suggests more for some deviations in the operational condition than deviations in the signal processing and parameter extraction. It should be noted that each case covers a period after a step change in the generator current, which might induce some perturbation into the final equilibrium state. In general and including the high load cases, the OMA is believed to produce more consistent damping data, as also indicated by the reasonably small deviation between the cases in Table 6.

Case	$\Delta T$ , sec.	% Rated Power	TNF1		TNF2	
			Hz	%	Hz	%
1.	43	1.1	14.7	0.51	36.8	0.49
2.	79	11.8	14.5	0.87	35.5	0.27
3.	90	27.1	14.7	0.57	35.9	1.06

**Table 5. Modal frequencies and damping ratios (pct. of critical damping) extracted from the shaft torque strain-gauges during steady state using OMA SSI methods**

Case	$\Delta T$ , sec.	% Rated Power	TNF1		TNF2	
			Hz	%	Hz	%
1.	134	1.1	14.7	0.61	36.8	0.59
2.	105	1.4	14.7	0.73	36.7	0.48
<b>Avg.:</b>	<b>119.5</b>	<b>1.3</b>	<b>14.7</b>	<b>0.7</b>	<b>36.8</b>	<b>0.5</b>
3.	104	11.8	14.5	0.78	35.5	0.29
4.	55	11.1	14.6	0.41	35.4	0.24
5.	80	11.4	14.5	1.07	35.5	0.47
6.	94	11.4	14.4	1.45	35.6	0.75
<b>Avg.:</b>	<b>83.3</b>	<b>11.4</b>	<b>14.5</b>	<b>0.9</b>	<b>35.5</b>	<b>0.4</b>
7.	138	26.8	14.7	0.58	36.2	2.61
8.	374	27.1	14.7	0.61	36.1	2.05
9.	175	26.8	14.7	0.60	36.0	2.81
10.	124	26.8	14.7	0.45	36.0	2.37
<b>Avg.:</b>	<b>202.8</b>	<b>26.9</b>	<b>14.7</b>	<b>0.6</b>	<b>36.1</b>	<b>2.5</b>

**Table 6 - Modal frequencies and damping ratios (pct. of critical damping) extracted from the shaft proximity probes during steady state using OMA SSI methods**

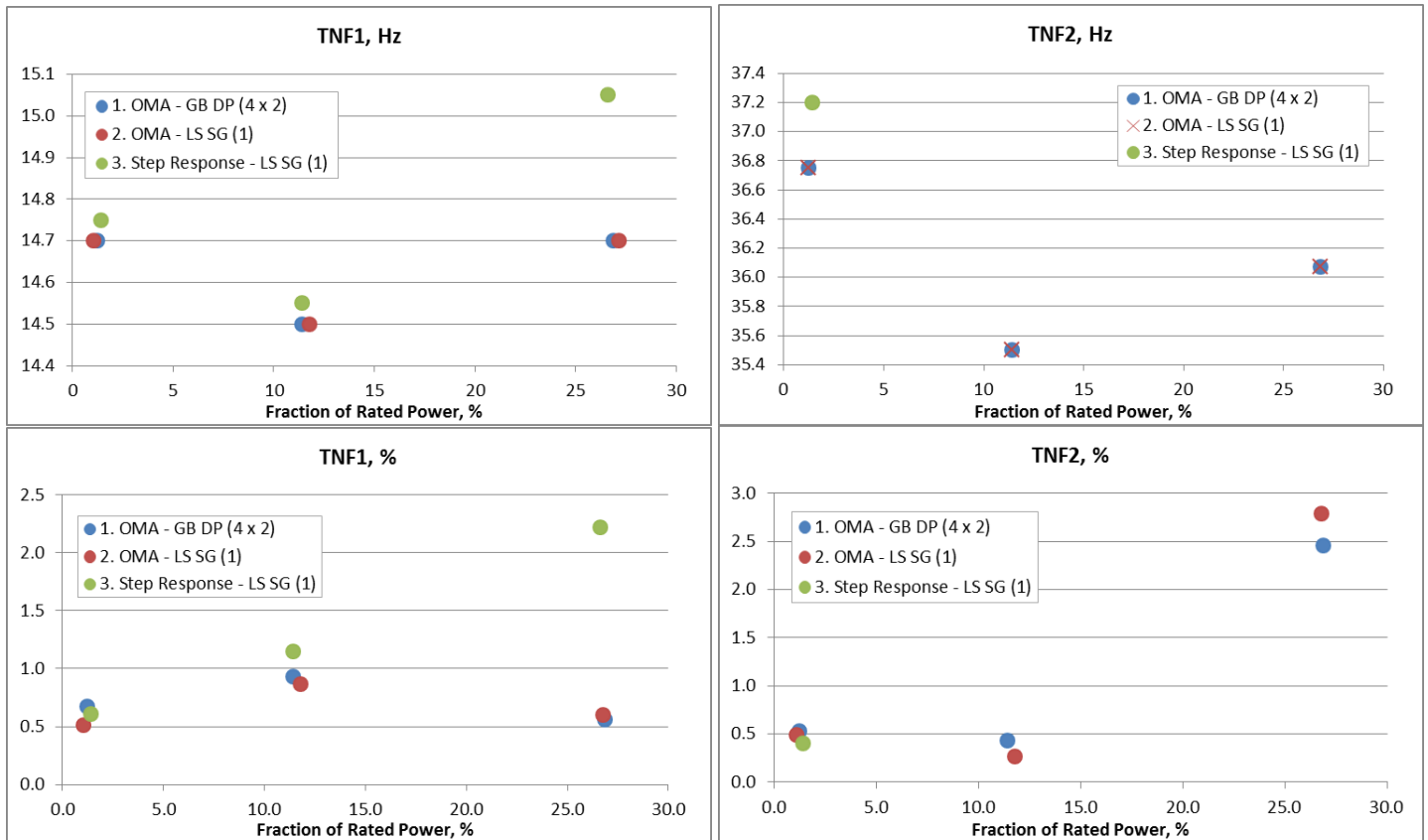


**Figure 23 - Graphical presentation of the estimates of the torsional modal frequencies and damping ratios, comparing results from the step response analysis and from the OMA of the shaft torque and the shaft displacement signals.**

### Conclusion from Case study 2

In this case study results from experimental determination of the modal parameters of the lowest two torsional vibration modes of a geared turbo-generator set have been presented. The modal parameters have been extracted using two methods:

1. Analysis of the step shaft torque response obtained from a range of electrical load step runs.
2. OMA on steady state data, by using shaft torque and also by using the 8 permanent shaft proximity probes from the gearbox.

The results showed that it was difficult to identify data for the second mode when using the load step approach, whereas it was possible to obtain consistent data at all load cases using OMA.

For the first torsional mode, the two methods showed good consistency for both the modal frequency and damping at the two low load scenarios at approx. 1% and 11% of rated power.

At the highest load case, approx. 27% of rated power, the step load method gave significantly deviating (higher) values for the modal frequency and damping, for the case where the step change was high, i.e. from approx. 1% to 27% rated

power. The non-linear properties of the fluid film bearings, caused by the eccentricity-dependent behavior for the stiffness and damping coefficients, are believed to contribute to this deviation during the movement of the shaft centerline during the load change.

When using the OMA method, the results extracted from the torque data were very similar to the data obtained using the proximity probes.

From the results, it can be concluded that using OMA on the gearbox proximity probes is very feasible for determination of the torsional modal data of a geared shaft train. The advantage of this method is that the parameters can be extracted in-situ during real operation conditions, without provision of expensive torque loading devices, such as the resistor load bank for this generator case, and cumbersome fitting of torquemeter devices.

The method could as well be incorporated as part of a condition monitoring system e.g. for monitoring coupling integrity and power turbine fouling.





**CASE STUDY 3: GAS TURBINE GENERATORS CONNECTED TO WEAK GRID**

Two 40+MW gas turbine driven generator (GTG) sets are connected to an islanded grid to which four large LCI type VSD motor driven compressor trains are connected; a high level schematics of the plant is given in Figure 24.

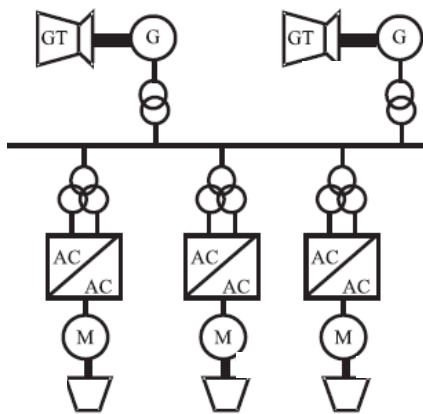


**Figure 24 – High level plant schematics of the plant.**

During commissioning of the compressor trains, the GTGs tripped on numerous occasions due to high vibrations in the gearbox lateral proximity probes.

A troubleshooting / root cause analysis was initiated. It started with frequency analysis of the GTGs gearbox proximity probe measurements, where a dominant subsynchronous frequency at approx.. 12 Hz was noticeably excited and ultimately caused trips, see Figure 25.

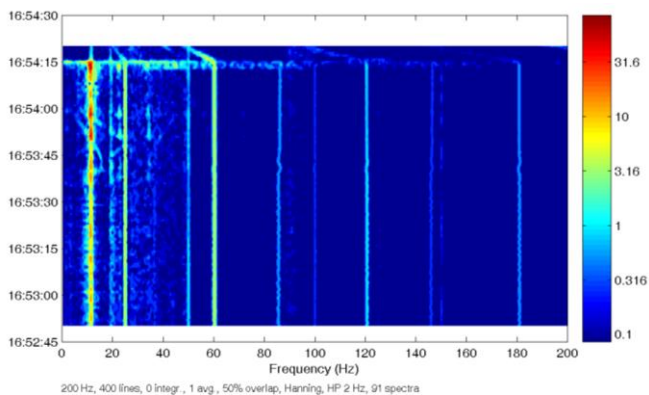


**Figure 25 - the proximity measurements on the generator at trip, dominated by a subsynchronous 12 Hz component.**

**Prediction of system torsional natural frequencies**

The subsynchronous vibration of interested was quickly identified as the first torsional natural frequency of the gas

generator train.

The torsional dynamics of the system is described in the following paragraph, where the results of a coupled torsional-lateral analysis are presented.

The turbine is driving the generator via a speed increasing gear box. The schematics of the genset are shown in **Figure 4**Figure 26.

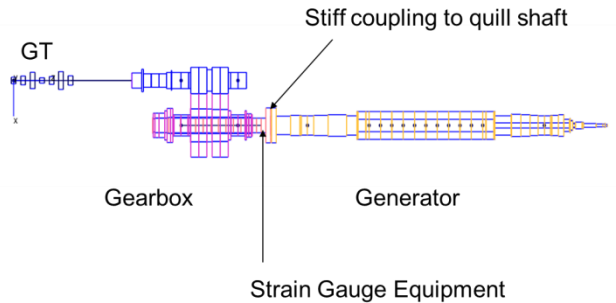


**Figure 26 – Outline of the torsional dynamic system. From left to right: Gas turbine, pinion gear (higher center), bull gear (lower center), generator (right).**

The calculated lowest natural frequencies are found in Table 7. The torsional Campbell diagram is presented in Figure 27.

Mode	Frequency [Hz] (Torsional)	Frequency [Hz] (Coupled)
1	12.06	12.04
2	19.59	19.58
3	42.28	42.17
4	55.90	55.89
5	104.2	104.2

**Table 7 - Calculated natural frequencies, torsional only and torsional-lateral coupled analysis**

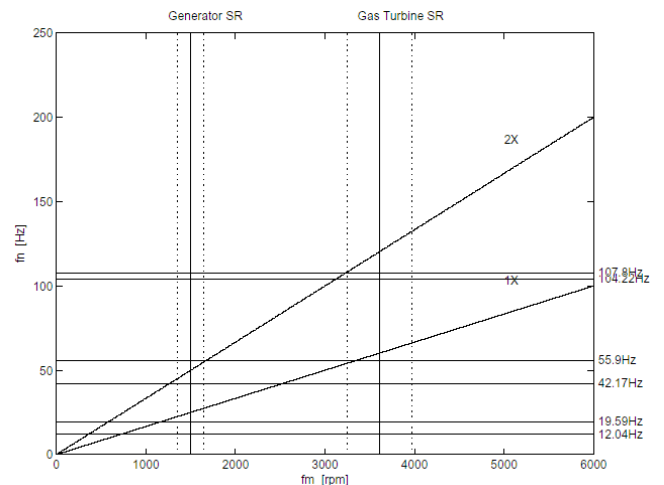


**Figure 27-Campbell diagram of torsion natural frequencies.**



### Troubleshooting

Initially, the troubleshooting concentrated around the possibility that the damping of the first torsional mode were so low that it became unstable under certain operating conditions.

The root cause analysis pointed towards following most likely scenarios:

- Low mechanical damping of the first torsional natural frequency making it sensitive to electrical damping induced instability, ref Figure 28.
- Generator AVR control loop settings having a negative influence on the damping.
- The role of electrical damping effect from the power network of the plant coupled to the generator via electromagnetic coupling.

All the possible root causes are very dependent on a good estimation of the damping.

In this case study it will be shown how the use of OMA has provided the damping of the torsion modes which would help to confirm the root cause at an earlier stage of the failure investigation.

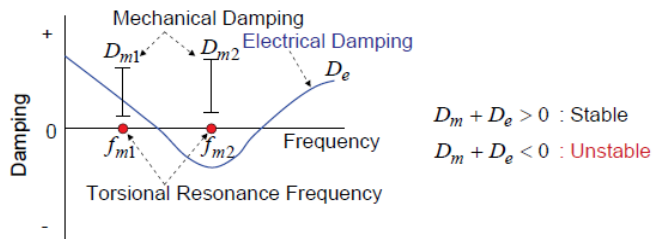


**Figure 28 – Illustration of combined mechanical and electrical damping on overall torsional stability of an electromechanical system, such as a GTG. From Fujii et al. 2013**

### Traditional measurements

In this case the damping was originally determined by the decay of the torsional natural frequency after a system trip. The damping is estimated on the basis of the free torque fluctuation after a load rejection on the generator. Figure 29 shows the torque fluctuation on the top plot and the 4-14 Hz band pass filtered torque on the bottom plot. The damping is estimated by fitting a single degree of freedom harmonic oscillation with damping to the band pass filtered torque curve. This is illustrated the bottom plot, which also shows two fitted curves with a damping equivalent to amplification factors of 20 and 25 respectively.

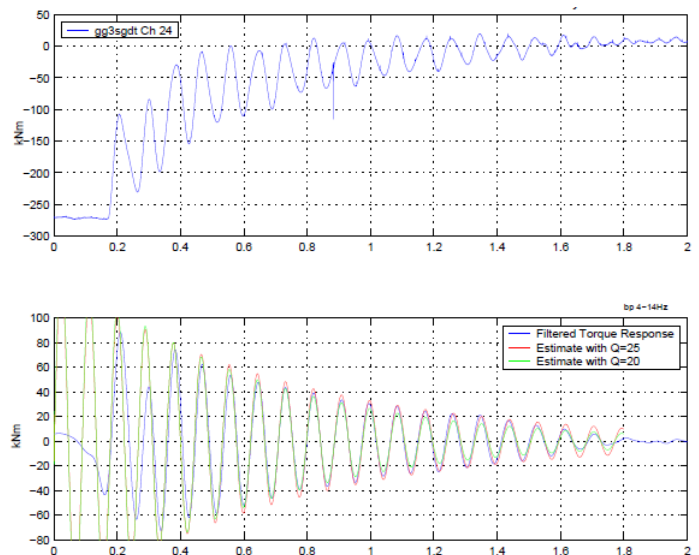


**Figure 29 - Torque fluctuation on the top plot and the 4-14 Hz band pass filtered torque on the bottom plot**

This damping estimate is performed during a trip, where conditions are very different compared to an operational situation. For example, absence of the load will influence the bearing dynamic coefficients; the generator is disconnected to from the grid and the AVR system is not active.

In short, this approach leaves the suggested root causes at almost the same uncertainty as before the damping was estimated.

### Modal properties from OMA

OMA analysis has been performed during four load cases at 0 (idle), 35, 40.5 and max load 45.5 MW. The length of the time interval for each analysis is 2 minutes due to the limitation in available measurement data. Two minutes corresponds to 1400 periods which is more than the 1000 periods required for an OMA, however longer measurements allow for more consistent results; it is as mentioned always recommended to use longer than necessary time sequences if these are available.

Shaft vibration signals were taken directly from the Bentley Nevada acquisition unit installed on site.

A total of 8 radial proximity probe data have been used for the OMA analysis, 2 for each pinion and bull gear shafts Drive End (DE) and Non-Drive End (NDE) proximity probes.

OMA has been used to identify the 1st, 2nd and 3rd Torsional Natural Frequencies (TNF) and the relative damping ratios. The results of the analysis are summarized in Table 8 and Figure 30 - Figure 32.



Power	TNF1		TNF2		TNF3	
	Hz	%	Hz	%	Hz	%
0	12.9	2.85	19.6	0.30	42.5	2.63
35	11.8	1.07	19.5	0.45	41.1	1.21
40.5	11.8	1.04	19.5	0.62	41.1	0.77
45.5	11.8	1.50	19.5	0.73	41.1	0.62

Table 8- OMA frequency and damping results for the first three torsion natural frequencies.

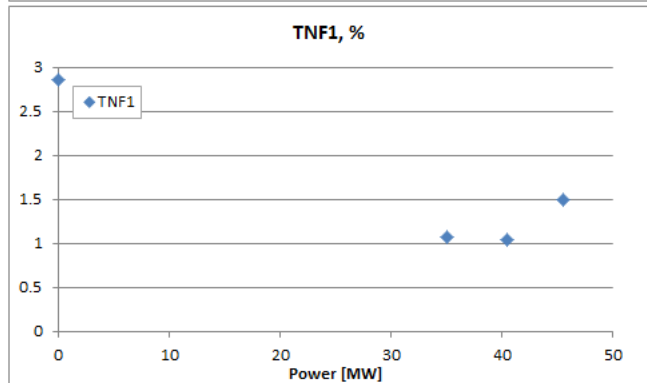
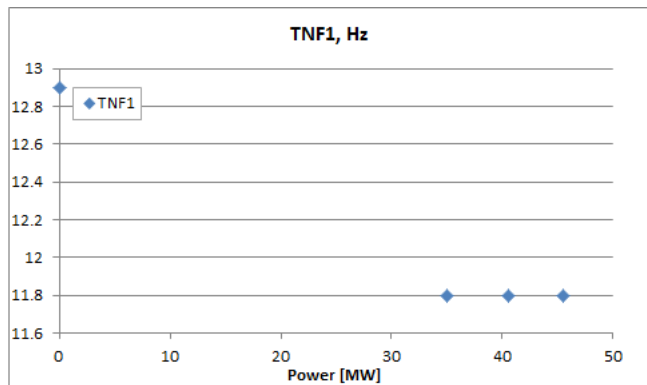


Figure 30- First torsion mode.

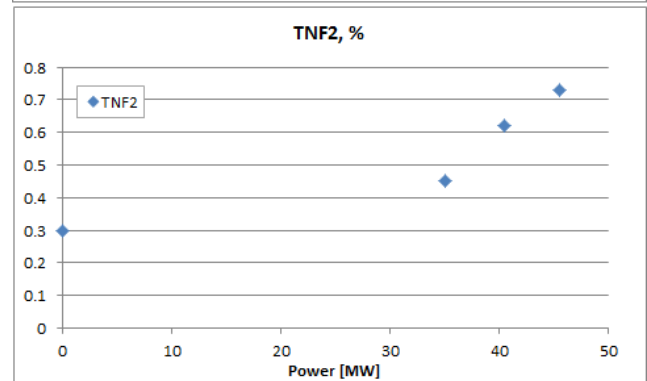
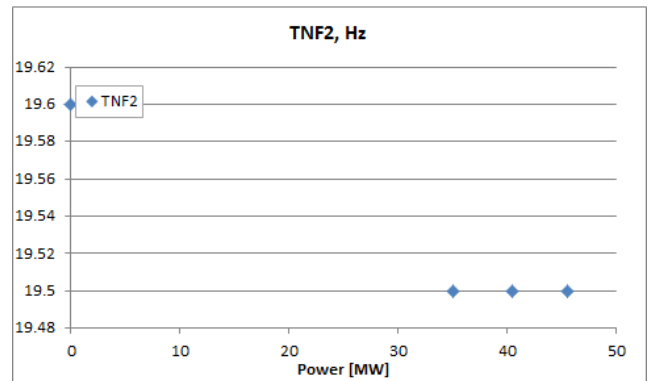


Figure 31- Second torsion mode.

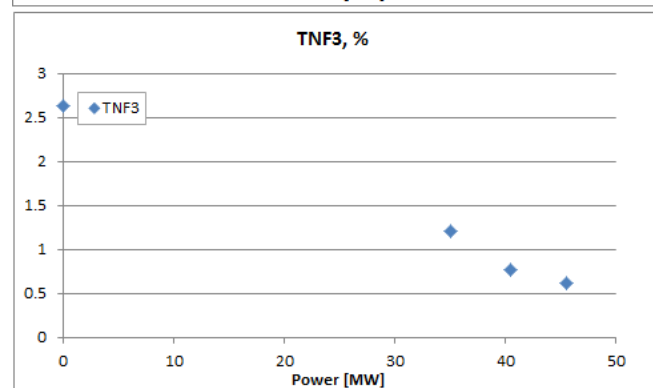
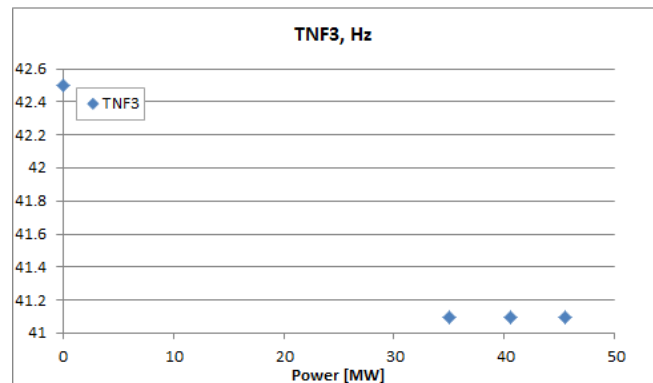
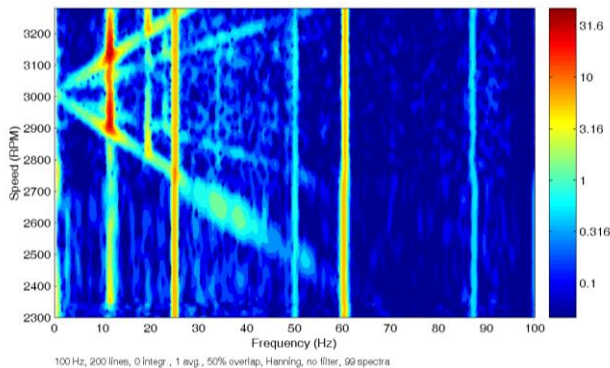


Figure 32 - Third torsion mode.



### Conclusions from Case study 3

An extensive description of the root cause analysis process is outside the scope of this work; however, ultimately it was determined that the first torsional natural frequency of the system was being excited not because of a negative torsional electromechanical damping, but by an electrical network frequency modulation component excitation, coupled to the torsional dynamics via the electromagnetic field of the generator. This frequency component was found to be connected to one of the VSD driven compressor being commissioned. In combination with a small island grid it is found a direct correlation between the gearbox vibration-levels and the motor speed on the VSD motor, Figure 33. It is evident that the trip is directly correlated to a certain operation interval of the VSD, where interharmonic torque pulsations are generated.



**Figure 33 - Contour plot of the GTG gearbox vibration plotted against the speed of the VSD compressor train being commissioned.**

OMA analysis excluded the assumption that the system is unstable during operation independent of both the influence of the voltage control systems and the stability of the grid. The torsional damping was however found to be relatively low and sensitive to excitation.

In order to come to these conclusions it is essential to have a good estimation of the systems damping during operation. This is a relatively easy task with the use of OMA compared to other existing methods.



## CONCLUSIONS

In this paper it has been demonstrated how Operation Modal Analysis (OMA) can be used to provide torsional damping estimation of geared rotating machinery using radial proximity data only.

OMA identifies the modal parameters of a system from measurement of response due to excitation with some unknown characteristics and is a mature technology applied outside of the field of rotor dynamics.

**In case study 1**, OMA has been applied to an electric driven compressor train. It has been shown how operational modal analysis can identify the modal parameters of a system over most of its typical operational range from measurements of response due to unmeasured excitation.

Parameter estimation obtained with proximity probe data proved to be reliable, at least as much as with dedicated torsional vibration recording equipment. This means that detailed torsional dynamics of geared turbomachinery can be evaluated with OMA algorithms with the sole use of readily available vibration data.

Acquiring such information during commissioning can be seen as a reference point for future surveys and better understanding of the root cause of deviations from the baseline behavior.

**In case study 2**, OMA has been applied to investigate the torsional behavior of a gas turbine generator set, comparing the results to those of traditional experimental modal analysis. The results showed that it was difficult to identify data for the second mode when using the load step approach, whereas it was possible to obtain consistent data at all load cases using OMA.

From the results we find it very feasible using OMA on the gearbox radial proximity probes for determination of the torsional modal data of a geared shaft train. The advantage of this method is that the parameters can be extracted in-situ during real operation conditions, without provision of expensive torque loading devices, such as the resistor load bank for this generator case, and cumbersome fitting of torque meter devices.

It was argued that the method could as well be incorporated as part of a condition monitoring system e.g. for monitoring coupling integrity and power turbine fouling.

**In case study 3**, OMA has been applied for troubleshooting gensets tripping during a plant commissioning. Analysis excluded preliminary assumptions that the torsional system was unstable during operation independent of both the influence of the voltage control systems and the stability of the grid. The torsional damping was however found to be relatively low and sensitive to excitation.

It was argued that in order to come to these conclusions it is essential to have a good estimation of the systems damping during operation. This is a relatively easy task with the use of OMA compared to other existing methods.

Traditional identification techniques of torsional modes rely step/impulse response or on sweeps through the available speed range. OMA provides a complementary technique to such analysis. In cases where the torsional mode lies at the edge or outside the operational speed range or is not well excited during the sweep, due to the speed with which the machine is run-up for example, then the traditional approach will struggle. OMA has the advantage that identification of torsional modes can be made with data acquired when the machine is running in a steady operational condition.

Moreover, it has been shown how common assumptions made during the design stage regarding torsional damping can be verified and model tuning can be performed thanks to the identified parameters.

The results suggest that interpretation of measured torsional modes at single instances, at stand still, off-load or at different certain load conditions should be treated with caution in terms of drawing general conclusions of torsional behavior. Knowledge of the torsional modes in operation can allow optimization of asset usage by avoidance of operational ranges which significantly excite the modes. OMA provides a significant benefit in investigating and understanding torsional behavior of rotors in operation.

On a broader perspective, just like OMA has been proved as a successful tool for large civil engineering structures, this paper aimed at demonstrate how it can be used to extract torsional dynamic information from a rotordynamic system. Potential applications include:

### **Design Model Validation**

OMA can be an invaluable tool since the very beginning of the operational history of a machine, where its dynamics properties can be assessed in the actual operation conditions and reconciled with those predicted in design.

### **Reference Point for Future Operation**

It is important to perform an initial assessment of the characteristics of a machine and its interaction with a structure. This reference point is essential for future surveys and better understanding of the root cause of deviations from the baseline behaviour.

### **Non-destructive Testing & Online Diagnostics**

Non-destructive testing is at the core of health monitoring systems, where the behavior of a machine is continuously monitored over time. In this case OMA presents a great advantage compared to other tools, since the system is observed during operation when often only stochastic/operational excitation sources are available.



## REFERENCES

- Avitabile, P. 2002 “Back to basics”. Experimental Techniques, Volume 26, Issue 2, pages 13–14.
- Brincker, R., and Andersen, P. 2001 “Damping estimation by frequency domain decomposition”. IMAC XIX, Kissimee, USA.
- Brincker, R., Zhang, L., and Andersen, P. 2000 “Modal identification from ambient responses using frequency domain decomposition”. Proc. of the 18th IMAC, San Antonio, TX, USA.
- Cantieni, R. 2013. “Experimental modal analysis under ambient excitation: what can we learn from experience”. In 5th International Operational Modal Analysis Conference, Portugal. Keynote.
- Carden, E.P., 2013. “Investigation Of Offshore Diesel Generator Failure Using Operational Modal Analysis”, in 5th International Operational Modal Analysis Conference, Portugal. Paper ID #135.
- Carden, E. P., and Lindblad, M., 2014, “Operational Modal Analysis Of Torsional Modes In Rotating Machinery,” Proceedings of ASME Turbo Expo 2014: Turbine Technical Conference and Exposition, June 16 – 20, 2014, Düsseldorf, Germany.
- Carden, E. P., and Morosi, S., 2014, “Operational Modal Analysis Of Lateral Rotordynamic Modes Of Rotating Machinery,” Proceedings of ASME Turbo Expo 2014: Turbine Technical Conference and Exposition, June 16 – 20, 2014, Düsseldorf, Germany.
- Carden, E. P.; Sehlstedt, N; Nielsen, K. K.; Lundholm, S; Morosi, S. “Stability analysis and assessment of rotor trains using operational modal analysis” Proceeding of 9th IFToMM International Conference on Rotor Dynamics, IFToMM ICORD 2014, Milan, Italy (2014)
- Clarke, H., Stainsby, J., Carden, E. P. 2011. “Operational modal analysis of resiliently mounted marine diesel generator/alternator”. In 30th International Modal Analysis Conference, USA.
- Eshelman, R. L. 1977 “Torsional Vibration of Machine Systems” Proceedings of the Sixth Turbomachinery Symposium.
- Felber, A. J., 1993. “Development of a Hybrid Bridge Evaluation System”. PhD thesis, University of British Columbia, Vancouver, Canada, December 1993.
- Fujii, T., Masuda H., Ogashi, Y. Tsukakoshi, M. Yoshimura, M. 2013 “Comparison between electrical drives in LNG plant for subsynchronous torsional interactions”, Proceedings of thLNG17, Houston
- Guglielmo, A., Mitaritonna, A., Catanzaro, M. and Libraschi, M. “Full Load Stability Test (FLST) on LNG Compressor”, Proceedings of ASME Turbo Expo 2014: Turbine Technical Conference and Exposition, June 16 – 20, 2014, Düsseldorf, Germany
- Hamrock, B.J. 1991 “Fundamentals of Fluid Film Lubrication” NASA reference publication 1255
- James, G. H., Carne, T. G., Lauffer, J. P., and Nord, A. R. 1992 “Modal testing using natural excitation”. Proceedings of the International Modal Analysis Conference .
- Ljung, L. 1999 “System Identification - Theory for the User” second ed. Information and System Science. Information and System Science Series. Prentice Hall.
- Maeck, J., 2003, Damage Assessment of Civil Engineering Structures by Vibration Monitoring, PhD Thesis, University of Leuven, ISBN 90-5682-390-6.
- Peeters, B., De Roeck, G., 1999 “Reference-Based Stochastic Subspace Identification For Output-Only Modal Analysis.” Mechanical Systems and Signal Processing 13(6), 855-878
- Peeters, B., Manzato, S., and Van der Auweraer, H., 2013 “Solutions to deal with harmonics and noise for helicopter in-flight data dynamic identification. In: 5th International Operational Modal Analysis Conference, Portugal, paper ID #241.
- Purup, N. B. 2014. “Operational Modal Analysis Applied to Structural and Rotor Dynamics – Theoretical and Experimental Aspects”, MSc thesis DTU - Technical University of Denmark.
- Rubin, S., 1981. “Ambient vibration survey of offshore platform”. Applied Oceanic Research 3, 2, 89.
- Van Overschee, P., and De Moor, B., 1996 “Subspace Identification for Linear Systems”. Kluwer Academic Publishers, USA .



44<sup>TH</sup> **TURBOMACHINERY** & 31<sup>ST</sup> **PUMP SYMPOSIA**  
HOUSTON, TEXAS | SEPTEMBER 14 – 17 2015  
GEORGE R. BROWN CONVENTION CENTER

Wachel, J.C. and Szenasi, F.R. 1993 “Analysis of Torsional Vibrations in Rotating Machinery”, Proceedings of the Twenty-Second Turbomachinery Symposium.

Wang, Q., Feese, T.D., Pettinato, B.C., 2012, “Torsional natural frequencies: measurement vs. prediction”. In Proceedings of the Forty-First Turbomachinery Symposium, September 24-27, Houston Texas.

Zhang, L., Wang, T., and Tamura, Y. 2010 “A frequency-spatial domain decomposition (fsdd) technique for Operational Modal Analysis” Mechanical Systems and Signal Processing, vol. 24, no. 5, pp. 1227-1239

Zhang, L., Brincker, R., and Andersen, P. 2005 “An overview of operational modal analysis: Major developments and issues”. Tech. rep., Nanjing University of Aeronautics and Astronautics, 2005.for operational modal analysis. IOMAC, Copenhagen, Denmark.

## NOMENCLATURE

$\Gamma_n$	= Hankel matrix
$n$	= system order
$U$	= left singular vectors
$V$	= right singular vectors
$S$	= singular values
$O_n$	= observability matrix of order $n$
	Moore-Penrose pseudoinverse
	$O_n$ without the last $L$ rows
	$O_n$ without the first $L$ rows
$A$	= dynamic matrix
$\lambda_d$	= eigenvalue of $A$ in discrete time
$\lambda_c$	= equivalent of $\lambda_d$ in continuous time
$\Delta t$	= sampling period

## ACKNOWLEDGEMENTS

The authors would like to thank the Engineering Dynamics group at Lloyd’s Register Consulting for the support to the project, in particular to the Machinery Dynamics Technology Leader Henning Hartmann for his time and suggestions.